Anatomically accurate, finite model eye for optical modeling

Hwey-Lan Liou and Noel A. Brennan

Department of Optometry and Vision Sciences, University of Melbourne, Parkville VIC 3052, Australia

Received July 19, 1996; revised manuscript received January 9, 1997; accepted January 23, 1997

There is a need for a schematic eye that models vision accurately under various conditions such as refractive surgical procedures, contact lens and spectacle wear, and near vision. Here we propose a new model eye close to anatomical, biometric, and optical realities. This is a finite model with four aspheric refracting surfaces and a gradient-index lens. It has an equivalent power of 60.35 D and an axial length of 23.95 mm. The new model eye provides spherical aberration values within the limits of empirical results and predicts chromatic aberration for wavelengths between 380 and 750 nm. It provides a model for calculating optical transfer functions and predicting optical performance of the eye. © 1997 Optical Society of America
[S0740-3232(97)01407-5]

1. INTRODUCTION

Recent advances in biometric measurement of the eye and in computerization to expedite extensive, complex optical calculations have made it possible to model the optical performance of the eye accurately. Predicting optical image quality at various levels of defocus, contrast, and pupil size can be achieved by calculation of modulation transfer functions from a model eye. This can be useful in estimating visual performance of those eyes undergoing refractive surgical procedures, such as photorefractive keratectomy and automated lamellar keratoplasty to correct ocular refractive errors. However, the choice of a suitable model eye for such calculation relies on its close conformity to the anatomical and optical characteristics of the human eye.

In calculating the modulation transfer function of the human eye in white light from experimental data on aberrations, van Meeteren[1] concluded that chromatic difference of focus and spherical aberration are the most important aberrations. A literature search to find a model eye that estimates both spherical aberration and chromatic aberration of the eye within the tolerances of empirical results was unsuccessful. A review of the spherical aberration predicted by model eyes[2] revealed that present schematic models estimated spherical aberration values that were higher than empirical results. Of these, only the model of Navarro *et al.*[3] provides estimates of chromatic aberration in addition to spherical aberration. The only model eye that has both aspheric surfaces and a gradient-index lens (Smith *et al.*[4]) gives estimates of spherical aberration that are higher than empirical results and does not provide values for chromatic aberration.

There is one model eye that accurately predicts spherical and chromatic aberration of the eye (provided that typographical errors in the paper are rectified[8]), and this was proposed by Thibos and co-workers.[5–7] However, it is a reduced eye model and therefore not suitable for the purposes of modeling vision where one or more refracting surfaces of the eye is altered, as in the case of refractive surgical procedures. Nevertheless, it is a simple and efficient model for predicting spherical and chromatic aberration of the eye and should be used if there is no additional requirement.

As current model eyes are limited in their application for vision modeling, our aim in this study is to develop a model eye that can be used to predict visual performance under normal and altered conditions of the eye. The specific aims of the project are to develop a new finite model eye that

1. Represents the ocular anatomy as closely as possible, so that it can be used in future modeling of visual performance in which one or more surfaces are altered;
2. Predicts spherical and chromatic aberrations as close to empirical results as possible, so that it can be used to predict optically dependent functions such as modulation transfer functions of the eye.

2. METHOD

We developed a new finite model eye by adopting empirical values of ocular parameters to produce a model structurally similar to the human eye. Then we modeled those parameters that lack experimental results or accuracy to give values for spherical and chromatic aberration that are close to empirical data. We reviewed the literature on the biometry of the eye and examined parameters such as axial length, anterior chamber depth, curvature and asphericity of refracting surfaces, gradient-index structure of the lens, and dispersion of the ocular media. Data adopted in our new finite schematic model were selected according to the following criteria:

1. Data used were obtained from healthy emmetropic eyes.
2. An average of 45 years was used if the parameter was age dependent. This choice of age was based on an adult life extending from approximately 20 to 70 years of age and the onset of presbyopia at about 45 years of age.

3. Results from *in vivo* experiments were chosen in preference to *in vitro* studies.

4. All other factors being the same, data from the most recent study and/or with the larger sample size were used.

Once the necessary biometric data were compiled, we identified those parameters that lacked empirical results or accuracy and used them as modeling variables. For paraxial calculations, curvature and gradient-index parameters were modeled with the aim of producing an eye with an equivalent power of 60 diopters (D) and an axial length of 24 mm. For finite calculations, asphericity parameters were modeled to produce spherical aberration values close to those found experimentally. The change in refractive index with wavelength was modeled to predict chromatic aberration of the eye.

3. SELECTION OF BIOMETRIC DATA

A. Intraocular Distances

Intraocular distances refer to the various distances between optical refracting surfaces within an eye; these include anterior chamber depth, thickness of the cornea and lens, vitreous depth, and the overall axial length.

Consistent values of axial length of the eye have been determined by various studies. In 1948 Stenström[9] reported mean values of axial length of 24.04 mm for males and 23.89 mm for females. The difference in gender has been confirmed by various other investigators,[10–12] with mean axial length values of approximately 24 mm for males and 23–24 mm for females. Table 1 lists the experimental results found by Stenström,[9] Jansson,[10] Yu *et al.*,[11] and Koretz *et al.*[12]

Anterior chamber depth and lens thickness appear to be age dependent. Jansson[10] found that the mean anterior chamber depth for males decreases from 3.86 mm at age 20–29 years to 3.58 mm at age 40–49 years. Similar findings were obtained by Leighton and Tomlinson[13] and Koretz *et al.*[12] The reverse was noted for lens thickness, which was found to increase in thickness with age.[12,13] Numerous other studies have been done on the anterior chamber depth and lens thickness. Fontana and Brubaker,[14] Leighton and Tomlinson,[13] Larsen,[15] Weekers and Grieten,[16] and many others have measured the depth of the anterior chamber. Clemmensen and Luntz,[17] Jansson,[10] Leighton and Tomlinson,[13] Koretz *et al.*,[12] and others have measured the lens thickness.

We chose to adopt results of intraocular distances from the investigation by Koretz *et al.*,[12] following the criteria detailed above and because their single study provided all the various intraocular distances of the eye. They made measurements on 32 males and 68 females. To give equal weights to gender, the average of male and female results were used rather than the mean value reported for all 100 subjects. The thickness of the central cornea was taken to be 0.50 mm as found by subtracting the vitreous depth, lens thickness, and anterior chamber depth from the length of the globe. This value was used rather than the value of 0.47 mm directly measured in the Koretz *et al.*[12] study, as various other studies on corneal thickness alone found results equal to 0.49 mm or larger.[18–21]

The thickness of the peripheral cornea is usually larger than that of the central cornea. However, measurement techniques and distance from center at which it has been measured are variable, and results vary from 0.6 to 0.7 mm at 15° from the center to the limbal periphery.[20,22–24] Therefore these were not used in the modeling but rather were used to check the order of magnitude of the modeled peripheral corneal thickness.

B. Cornea

There are many ways of describing an aspheric surface. A common method is to use a conicoid in the form

$$x^2 + y^2 + (1 + Q)z^2 - 2zR = 0, \tag{1}$$

where the origin is chosen at the surface's apex, x is the horizontal meridian, y is the vertical meridian, z is the axis of revolution, R is the radius at the apex, and Q is the asphericity parameter that specifies the type of conicoid.

This representation of the cornea is rotationally symmetric and does not allow meridional variations in the values of R (i.e., astigmatism) or Q unless otherwise modified. In a study of ocular refraction in young men for the British National Service, Sorsby *et al.*[25] found that some 80% of 1680 eyes showed spherical refractions with less than ± 0.5 D of astigmatism. Given that the cornea accounts for the majority of the refracting power of the eye, it is reasonable to assume that we can represent the cornea as a rotationally symmetric conicoid for the purpose of an eye model.

As shown in Table 2, early investigations[9,26] measured anterior central corneal radius only, and some studies[27,28]

Table 1. Axial Length Measurements Reported by Various Investigators

Author	Year	Method	Gender	Number of Eyes	Axial Length Measurements (mm)
Stenström[9]	1948	Roentgenology	Male	685	24.04
			Female	315	23.89
Jansson[10]	1963	Ultrasonography	Male	113	24.00
			Female	71	23.14
Yu *et al.*[11]	1979	Ultrasonography	Male	1749	23.76
			Female	40	23.74
Koretz *et al.*[12]	1989	Ultrasonography	Male	32	24.08
			Female	68	23.42

Table 2. Summary of Experimental Results on Anterior Corneal Radius and Asphericity

Author	Year	Number of Eyes	Radius (mm)	Asphericity (Q)
Townsley[27]	1970	350	—	−0.30
Mandell and St. Helen[28]	1971	8	—	−0.23 (−0.40 to −0.72)
Stenström[9]	1948	1000	7.86 (7.00 to 8.65)	—
Sorsby *et al.*[26]	1957	194	7.79 ± 0.27	—
Kiely *et al.*[29]	1982	176	7.72 ± 0.27	−0.26 ± 0.18
Guillon *et al.*[31]	1986	220	7.77 ± 0.25	−0.19 ± 0.16 (steep meridian) −0.17 ± 0.15 (flat meridian)

Table 3. Summary and Comparison of Results on Anterior and Posterior Corneal Radii of the Same Eyes

Author	Year	Number of Eyes	Method	Comments	Anterior radius (A) (mm)	Posterior radius (P) (mm)	Ratio of A/P
Lowe and Clark[32]	1973	92	Slit lamp	Age 23–77 Mean Age=61.4	7.65 ± 0.27	6.46 ± 0.26	$P = 0.791A + 0.409$
Royston *et al.*[33]	1990	15	Slit lamp		7.77	6.35	1:0.817
			Purkinje image		7.77	6.40	1:0.824
Dunne *et al.*[34]	1992	80	Purkinje image	Refractive error range = −16.5 D to +4.7 D	7.98 (male) 7.84 (female)	6.44 6.36 (Spherical component only)	1:0.823
Patel *et al.*[36]	1993	20	Calculation using anterior corneal surface			5.8	

in the 1970's concentrated purely on asphericity of the anterior corneal surface without reference to the apical corneal radius. In 1982 Kiely *et al.*[29] calculated values for both corneal radius and asphericity, using the conicoid representation. Using an autocollimating keratoscope developed by Clark,[30] Kiely *et al.*[29] measured the anterior corneal shape of 176 healthy eyes. They found a mean value of 7.72 ± 0.27 mm for the central radius R and −0.26 ± 0.18 for the asphericity Q. In 1986 Guillon *et al.*[31] repeated a similar experiment but used a keratometer to measure the central cornea and a commercially available photokeratoscope for the peripheral cornea. Two hundred and twenty eyes representative of a normal population were studied and gave a mean value of 7.77 ± 0.25 mm for the central corneal radius R, $Q = -0.17 \pm 0.13$ for the flat meridian and $Q = -0.19 \pm 0.16$ for the steep meridian.

In a summary of nine papers dealing with central corneal keratometric values, Clark[30] reported a mean of 7.80 mm and a range from 7.0 to 9.0 mm for a healthy Caucasian population. Given that Guillon *et al.*[31] found a central corneal value (7.77 mm) closer to this average of 7.80 mm and that the study is more recent and has a larger sample size, the mean values of radius and asphericity reported in their study have been adopted for the new model eye.

Data on the curvature of the posterior corneal surface are scarce, but because of the much smaller refractive step, the curvature's effect is not very great. Table 3 is a summary of investigations on both anterior and posterior corneal radii and their comparison. In a series of studies done in 1973, Lowe and Clark[32] investigated the anterior and posterior corneal radii and their correlation. They measured mean values of 7.65 and 6.46 mm for the anterior and posterior corneal radii, respectively, and found the two parameters to be related as follows: posterior radius = 0.791 × anterior radius + 0.409.

In 1990 Royston *et al.*[33] investigated a new method of measuring the posterior radius using Purkinje images and compared it with the slit-lamp method used by Lowe and Clark.[32] They obtained similar results from the two methods; the average anterior corneal radius was found to be 7.77 mm with both methods, and the average posterior corneal radii were found to be 6.35 mm and 6.40 mm with the slit-lamp and the Purkinje image methods, respectively. The same authors then repeated a similar experiment on 80 eyes[34] and determined the ratio of anterior corneal radius to posterior corneal radius to be 1:0.823. This ratio is adopted in the new model eye to give a posterior corneal radius of 6.40 mm, given an anterior corneal radius of 7.77 mm.

To our knowledge, there are no direct measurements of the shape of the posterior corneal surface. Rivett and Ho[35] attempted to determine the shape of the posterior corneal surface by using data of anterior corneal surface and thickness. They found a Q value of −1.14 and −1.52 for the right and the left eyes, respectively. Patel *et al.*[36] tried similar calculations in 1993 and found Q values of −0.36 and −0.48 for the vertical (y) and horizontal (x) meridians of the posterior corneal surface. However, they measured the anterior corneal surface to be nearly spherical, and this differed from the usually accepted

value of asphericity, $Q = -0.18$ to -0.26, which probably affected their calculated value of posterior corneal asphericity.

Given that the posterior corneal asphericity is one of the more inadequately defined optical parameters of the eye, we entered it as a variable in the modeling of our model eye.

C. Lens

There are fewer studies on lens shape than on corneal shape because of the difficulties of measurement. Results obtained by various investigators vary considerably depending on the method used and whether measurements were taken *in vivo* or *in vitro* (see Table 4). Lowe and Clark[37,38] studied the anterior lens curvature in people with healthy and glaucomatous eyes. In a series of 92 normal eyes under cycloplegia from subjects aged 23–77 (mean age = 61.4), they found that the lens radius had a mean value of 10.29 mm with a range from 7.50 to 15.38 mm. The anterior lens radius correlated negatively with age, and the mean value was approximately 11.26 mm for 45 years of age. Similar results were obtained by Brown[39] in a series of 200 emmetropic eyes under cycloplegia in subjects aged 3–82 years. He found the mean central anterior lens radius to be 12.4 mm and the mean central posterior lens radius to be 8.1 mm. He also provided measurements of peripheral anterior and posterior lens radius. These are 13.3 mm and 7.1 mm at a distance of 2.8 mm and 2.4 mm from the center, respectively. Measurements of lens asphericity were made by Howcroft and Parker.[40] They found values of 7.3 mm and 5.35 mm for the anterior and posterior lens radii, respectively, and Q values of -3.13 and -1.0 for the anterior and the posterior lens asphericity, respectively. The lens radii measured by these two researchers are considerably less than those found by other authors, probably because they used cadaver lenses, which are likely to have undergone changes in lens shape after death.

In order to adopt a full set of *in vivo* results for both anterior and posterior surfaces and both radius and asphericity values, Brown's[39] measurements were chosen. The asphericity values for the anterior and posterior lens surfaces were obtained using the central and peripheral radius values provided by Brown, assuming a rotationally symmetric conicoid representation for the anterior and posterior surfaces.

The relation between the instantaneous tangential radius of curvature $\rho(y)$ and asphericity Q can be derived as follows. In the vertical (y) meridian the conic section is expressed by

$$y^2 + (1 + Q)z^2 - 2zR = 0. \tag{2}$$

In Cartesian coordinates, ρ can be derived with the general expression

$$\rho = \frac{[1 + (y')^2]^{3/2}}{y''}. \tag{3}$$

This yields

$$\rho = \frac{(R^2 - Qy^2)^{3/2}}{R^2} \tag{4}$$

or

$$Q = \frac{R^2 - (\rho R^2)^{2/3}}{y^2}. \tag{5}$$

These agree with equations obtained by Roberts[41] if Q is replaced by $Q = -e^2$, where e is eccentricity of the conic section. Inserting measurements of Brown[39] into Eq. (5) gives anterior and posterior lens asphericities of -0.94 and $+0.96$, respectively.

Measurements of the gradient refractive index of the lens are scarce. Nakao *et al.*[42] investigated the distribution of the refractive index in five lenses, using an interference technique on lens sections. Highest values of the lens refractive index were found at the center of the lens and varied from 1.403 to 1.409. There was intersubject variability in the distribution of the gradient index. Campbell[43] developed a nondestructive method for measuring the refractive index of intact crystalline lenses, and this method was used by Pierscionek and Chan[44] to study the gradient-index profiles in three human lenses aged 16, 56, and 84 years. Results of their measurements for the 16-year-old human lens were used in the modeling of the new model eye. Pierscionek and Chan[44] stated that their method of calculation necessitated an ac-

Table 4. Summary of Experimental Results on Anterior and Posterior Lens Radius and Asphericity

Author	Year	Number of Eyes	Method	Comments	Anterior Lens Radius (mm)	Posterior Lens Radius (mm)
Lowe[37]	1972	92	*in vivo*	Age 23–77	Mean = 10.29 ± 1.78 Range = 7.50 − 15.38	—
Lowe and Clark[38]	1973	92	*in vivo*	Mean age = 61.4 Same series as Lowe 1972[37]	Mean = 11.26 for 46 years of age	—
Brown[39]	1974	200	*in vivo*	Age 3–82 Emmetropia $< \pm 0.75_{DS}$ $< \pm 0.50$ cyl	Central 12.4 ± 2.6 Peripheral 13.3 ± 3.2	Central 8.1 ± 1.6 Peripheral 7.1 ± 1.4
Parker[70]	1972	100	*in vitro*	Mean age = 65 Range 12–91	Radius = 5 $Q = -1.5$	Radius = 3.3 $Q = -1.0$
Howcroft and Parker[40]	1977	120	*in vitro*	Age 1–87 Mean age = 51.4	Radius = 7.3 ± 0.3 $Q = -3.13$	Radius = 5.35 ± 0.14 $Q = -1.0$

curate estimate of the refractive-index value at the lens surface. Errors in this value will affect the profile values near the lens capsule but not those at the center. This means that their results are valid near the center but have increasing uncertainty at greater distances from the center.

D. Refractive Indices and Dispersion of the Ocular Media

We adopted a refractive-index value of 1.376 for the cornea following Gullstrand's[45] model eyes, because to our knowledge there are no recent studies on the corneal refractive index. Similarly, we adopted Gullstrand's refractive index of 1.336 for the aqueous and vitreous humors.

Experimental data on dispersion of the ocular media are scarce. Le Grand[46] used the Cornu formula to compute the refractive indices. Palmer and Sivak[47] and Sivak and Mandelman[48] attempted to provide some basic dispersion data of the ocular media for humans and other vertebrates. However, measurements of the human ocular media included only values for the lens capsule, lens core, and lens periphery, and the standard deviations of mean findings were significantly large. They found that the ocular refractive indices all increase rapidly at the violet end of the spectrum, and Cornu's formula cannot adequately represent this change in refractive index.

In experimental studies of the chromatic dispersion of the ocular media, Sivak and Mandelman[48] investigated the dispersion of the ocular media of various vertebrates, including humans. They found that, in general, the aqueous humor and the cornea have a dispersion similar to that of water, whereas the lens is significantly more dispersive than water. Given the lack of experimental data on dispersion of the human ocular media, these will be assumed to have dispersive properties similar to those of water in the modeling of the new model eye. The refractive indices presented above will be taken for the wavelength of 555 nm, which is the peak of the photopic V_λ curve.

E. Pupil

Anatomically, the pupil is positioned directly in front of the crystalline lens. It is not exactly centered with respect to the rest of the eye and is often displaced slightly nasally by ~0.5 mm.[49] Because of the various aberrations of the eye, this displacement has some effect on image quality and visual performance.

Recent research into pupil centration has revealed that it changes with change in illumination and pupil size.[50,51] Wilson *et al.*[50] measured the centration of the pupil with respect to the achromatic axis of the eye as a function of pupil size. They found significant shifts of the pupil center (up to 0.6 mm) with pupil dilation in both nasal and temporal directions. The effect was usually symmetrical between the two eyes, and the shift was linear in half of the subjects. Walsh[51] found changes in pupil centration of up to 0.4 mm in both natural and drug-induced pupil dilations. For the 39 subjects tested, there was no significant relationship between the direction of the change in centration occurring and the degree of natural pupil dilation in the dark. The mean (±SD) shift was very small (0.09 ± 0.17 mm temporal and 0.03 ± 0.15 mm inferior), although the mean absolute centration change (regardless of direction) was significant (0.19 ± 0.12 mm).

Walsh and Charman[52] investigated the effect of pupil centration and diameter on ocular performance. They found that while decentration caused relatively little difference in modulation transfer function at the smaller pupil size, it could produce marked degradations for the larger pupils.

Given the importance of the position of the pupil, the pupil was modeled as a circular aperture stop on the front surface of the lens with its center decentered 0.5 mm nasally from the optical axis. We did not model a change of pupil center with changing pupil size, in the absence of empirical data that specifies a consistent change.[50,51]

F. Angle Alpha

The visual axis of the human eye does not coincide with the optical axis, as the fovea is normally displaced temporally from the optical axis. We have adopted the definition of visual axis used by Bennett and Rabbetts[53] and others. In view of the meaning of visual axis, it is defined as the axis or chief ray of the actual pencil of rays that enters the pupil and is converged to the fovea. It therefore denotes the incident ray path directed toward the center E of the entrance pupil such that the conjugate refracted ray falls on the fovea. The angle between the optical axis and the visual axis is termed the angle alpha and is considered positive when the visual axis in object space lies on the nasal side of the optical axis. A positive value of approximately 5° is commonly found.[53] To our knowledge, no previous schematic eye has incorporated angle alpha into its model. We have included a 5° angle alpha in this new model, and this is used in image-quality calculations such as the modulation transfer function.

4. MODELING OF THE EYE

All optical calculations were performed with the CodeV™ optical design and analysis software from Optical Research Associates, Pasadena, Calif. Exact ray tracing was involved in all calculations.

From the examination and selection of biometric data, two parameters were identified as being inadequately defined by experimental results, namely, the posterior corneal asphericity and the gradient-index distribution of the lens. The latter affects paraxial parameters, while the former has an effect on the prediction of spherical aberration. We first modeled the distribution of the gradient index of the lens to produce an eye with the normally accepted equivalent power of 60 D (Ref. 45) and an axial length of 24 mm.

The circles in Fig. 1 represent the experimental data of Pierscionek and Chan.[44] The lens index is plotted as a function of r, which is the normalized distance from the lens center to the periphery. Because these data points have increasing uncertainty at greater distances from the lens center, we weighted the individual data points differently in the curve-fitting procedure. Weighting equals 1 at $r = 0$ (i.e., in the core of the lens), and weighting = 0 at $r = 1$ (i.e., at the lens surface). Different weightings were investigated for data points between $0 < r < 1$;

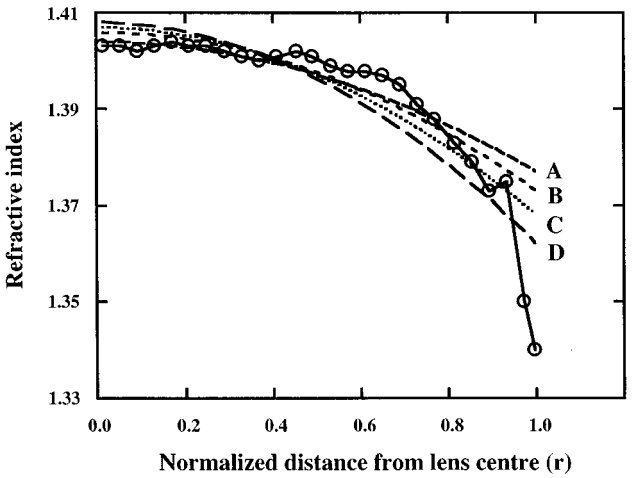

Fig. 1. Refractive-index distribution data of Pierscionek and Chan[44] (circles). The four parabolic curves represent the various smoothed-lens refractive-index distributions with different weightings given to the experimental data points. A, weight $= 1 - r$; B, weight $= \sqrt{1 - r}$; C, weight $= \sqrt[4]{1 - r}$; D, no weighting (i.e., weighting = 1 for all data points), where r is the normalized distance from the lens center.

these took the forms of $1 - r$, $\sqrt{1 - r}$, $\sqrt[4]{1 - r}$, and unity (i.e., not weighting), as they produced equivalent powers of the eye ranging from 58 to 62 D. The shape of the index distribution was assumed to be parabolic, as otherwise there exist an infinite number of higher-order possibilities for the mathematical form of a nonparabolic distribution, and there are not enough data to ascertain any particular higher-order form. Figure 1 shows the fitted parabolic curves for different weightings compared with the original experimental results. It is assumed that the variation of the lens index as a function of normalized distances is the same in the equatorial and sagittal planes. For simplicity of calculation, the lens is divided into anterior and posterior sections. The method of Smith *et al.*[4] is used to derive the thicknesses of the anterior and posterior sections and to convert the parabolic gradient-index distribution, expressed in normalized distance r, to one expressed in actual lens thicknesses. The distribution of the gradient index is represented in the form

$$n(w, z) = n_{00} + n_{01}z + n_{02}z^2 + n_{10}w^2, \qquad (6)$$

where z is along the optical axis, w is the radial distance perpendicular to the z axis ($w^2 = x^2 + y^2$), and n_{00}, n_{01}, n_{02}, and n_{10} are the index coefficients for a parabolic gradient-index distribution in an unaccommodated lens.

Because of the partition of the lens, we have introduced an imaginary plane surface between the anterior and posterior parts to demarcate the start of the posterior section. This surface has zero radius of curvature and no asphericity.

We have previously reviewed empirical results of the spherical aberration of the eye from various studies[2] and found that the relationship between longitudinal spherical aberration SA and ray height h can be best described by a linear model where SA $= 0.20h$ and the range is approximately ± 0.25 D from the value of spherical aberration for ray heights of up to 4 mm from the optical axis. The posterior corneal asphericity was modeled to predict spherical aberration of the eye by the above relationship. We investigated asphericity values between $Q = 0$ and -1.0 in steps of 0.2 for the posterior corneal surface. $Q = 0$ represents a spherical surface, $Q = -1$ is a paraboloid with the axis along the optical axis, and $-1 < Q < 0$ represent ellipsoids with the major axis along the optical axis.

To predict the chromatic aberration of the eye, we assumed the ocular media to have dispersive properties similar to those of water. Sivak and Mandelman[48] measured the variation of the refractive index of water with wavelength. We adopted their findings and fitted a curve to express the results as follows:

$$n \text{ (water)} = 1.3847 - 0.1455\lambda + 0.0961\lambda^2, \qquad (7)$$

where λ is in micrometers. Given that the refractive index of water is 1.3335 at 0.555 μm, Eq. (7) can be rewritten as

$$n \text{ (water at } \lambda \ \mu\text{m)} = n \text{ (water at 0.555 } \mu\text{m)} + 0.0512 - 0.1455\lambda + 0.0961\lambda^2. \qquad (8)$$

The various ocular media are assumed to have dispersive properties similar to those of water, and their refractive indices at various wavelengths λ can be found by replacing water by media as follows:

$$n \text{ (mediaa at } \lambda \ \mu\text{m)} = n \text{ (media at 0.555 } \mu\text{m)} + 0.0512 - 0.1455\lambda + 0.0961\lambda^2. \qquad (9)$$

For calculations of the modulation transfer-function (MTF), angle alpha was incorporated by using a pencil of rays directed toward the center of the entrance pupil at an angle of 5° nasally from the optical axis. We have denoted the nasal side of the optical axis to be positive, so angle alpha = +5° and pupil decentration = +0.5 mm (i.e., nasally, too).

5. RESULTS

Table 5 lists the equivalent power and the axial length of the model eye with different weightings. The $\sqrt[4]{1 - r}$ weighting of the gradient-index lens distribution gives an equivalent power of 60.35 D and an axial length of 23.95 mm, and this is used in the final eye model.

Table 5. Equivalent Power and Axial Length of the New Schematic Eye When Different Weightings of Data Points Are Used in Curve Fitting the Gradient-Index Distribution of the Lens

Weighting	Equivalent Power (D)	Axial Length (mm)
None (unity)	61.68	23.55
$\sqrt[4]{1 - r}$	60.35	23.95
$\sqrt{1 - r}$	59.19	24.31
$1 - r$	57.87	24.74

Figure 2 shows the spherical aberration predicted from the new model eye, with asphericity values of $Q = 0$ decreasing to -1.0 in steps of 0.2 for the posterior corneal surface. The best linear fit and range of spherical aberration obtained from compiling various experimental investigations[2] are shown for comparison. When the asphericity of the posterior corneal surface is $Q \geq -0.4$, the spherical aberration estimated from the model eye is less than the mean experimental data at all ray heights. Posterior corneal asphericity values of $Q < -0.6$ result in predicted values greater than the mean experimental data at 4 mm ray height, close to the mean experimental value at 2–3 mm ray height and less than this at 1 mm ray height. Of these, the curve describing spherical aberration using $Q = -0.6$ is the only one that lies entirely within the range of empirical results. We took this to be the curve best approximating the mean experimental spherical aberration, and the value of $Q = -0.6$ is adopted as the posterior corneal asphericity in the new model eye.

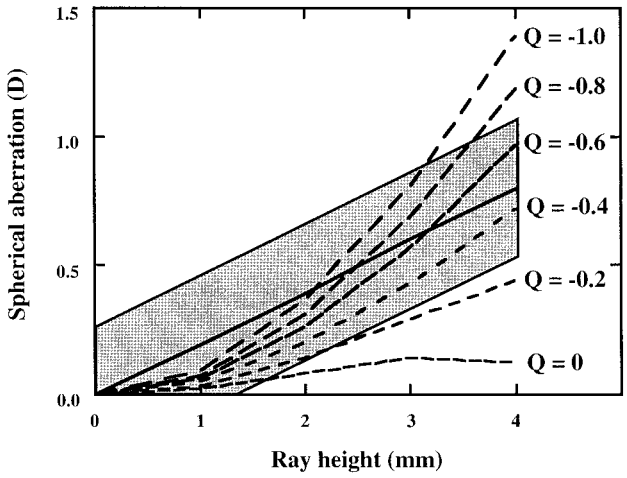

Fig. 2. Spherical-aberration values predicted by the new schematic eye, with various asphericity values Q for the posterior corneal surface (dashed curves) compared with the line of best linear fit (solid line) and range (shaded region) of empirical results.

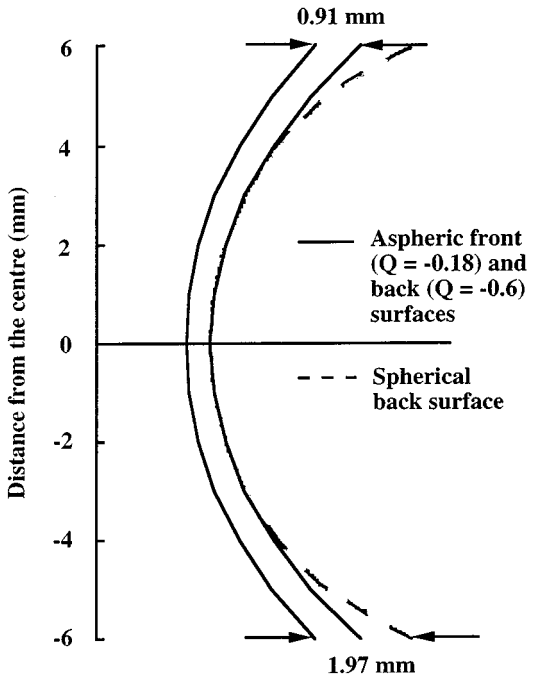

Fig. 3. Diagram showing the variation of corneal thickness given aspheric front and back surfaces.

Table 6. Structural Parameters of the New Schematic Eye

Surface	Radius	Asphericity	Thickness	n at 555 nm
1	7.77	−0.18	0.50	1.376
2	6.40	−0.60	3.16	1.336
3 (pupil)	12.40	−0.94	1.59	Grad A
4	Infinity	—	2.43	Grad P
5	−8.10	+0.96	16.27	1.336

The aspheric shape of the posterior corneal surface in combination with the aspheric front surface gives a thickness of 0.50 mm to the central cornea and 0.91 mm at a peripheral point 6 mm from the center (i.e., at the edge of a 12-mm cornea), the thickness gradually increasing from the center to the periphery (see Fig. 3). Had the posterior cornea been spherical, as assumed by most previous finite schematic models,[3,4,54–56] the peripheral cornea would have been thicker, with values as high as 1.97 mm at 6 mm from the center.

Table 6 lists all the parameters of the new proposed model eye, whose format can be readily used in any optical design and analysis software, and Fig. 4 illustrates the schematic features of the new proposed model eye and shows the directions of angle alpha and pupil decentration. Details regarding Table 6 are as follows. Surface 3 contains the pupil aperture whose center is decentered by 0.5 mm nasally. The aspheric surface 3 is still centered around the optical axis like all other surfaces, even though the pupil aperture is not centered. Surface 4 is an imaginary plane dividing the lens into anterior and posterior sections. The gradient index of the lens is described by $n(w,z) = n_{00} + n_{01}z + n_{02}z^2 + n_{10}w^2$, where z is along the optical axis, w is the radial distance perpendicular to the z axis ($w = x^2 + y^2$), and n_{00}, n_{01}, n_{02}, and n_{10} are the index coefficients for a parabolic gradient-index distribution in an unaccommodated lens. In grad A, $n_{00} = 1.368$, $n_{01} = 0.049057$, $n_{02} = -0.015427$, $n_{10} = -0.001978$; and in grad P, $n_{00} = 1.407$, $n_{01} = 0.000000$, $n_{02} = -0.006605$, $n_{10} = -0.001978$. The different ocular refractive indices at various wavelengths λ can be found as n (media at λ μm) $= n$ (media at 0.555 μm) $+ 0.0512 - 0.1455\lambda + 0.0961\lambda^2$.

In Fig. 5 the spherical aberration predicted by the new model eye is compared with the mean experimental results for spherical aberration. The spherical aberration estimated from the Gullstrand no. 2[45] and Le Grand[46] paraxial schematic eyes and the Kooijman[55] and Navarro *et al.*[3] finite schematic eyes are shown for comparison. The contribution of the gradient-index lens to the spherical aberration of the eye is shown in Fig. 6.

Applying Eq. (9) to obtain the refractive indices of different ocular media at various wavelengths resulted in a chromatic aberration close to experimental results

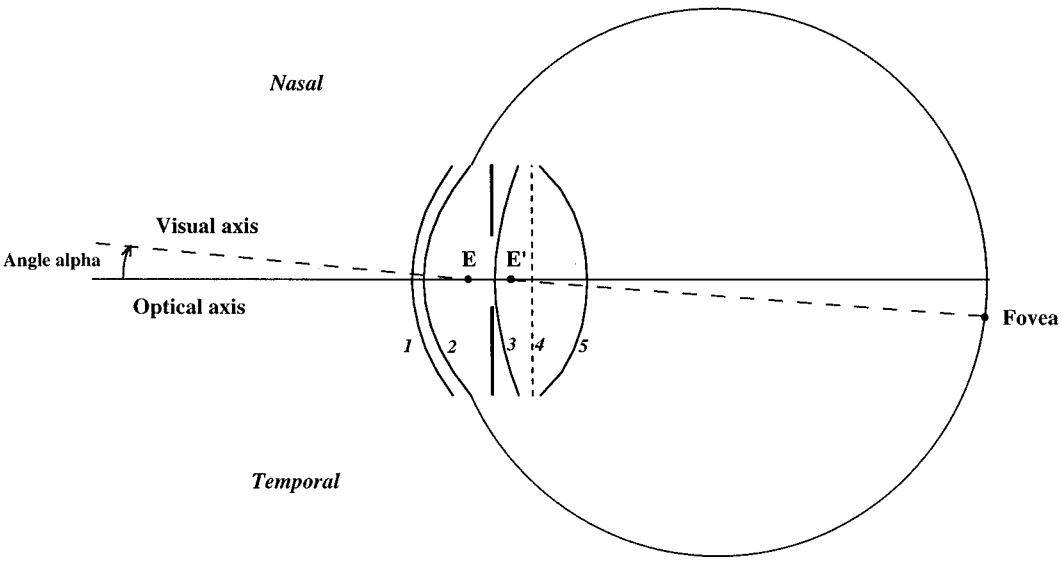

Fig. 4. Schematic drawing of the new schematic eye (see Table 6 for parameter values).

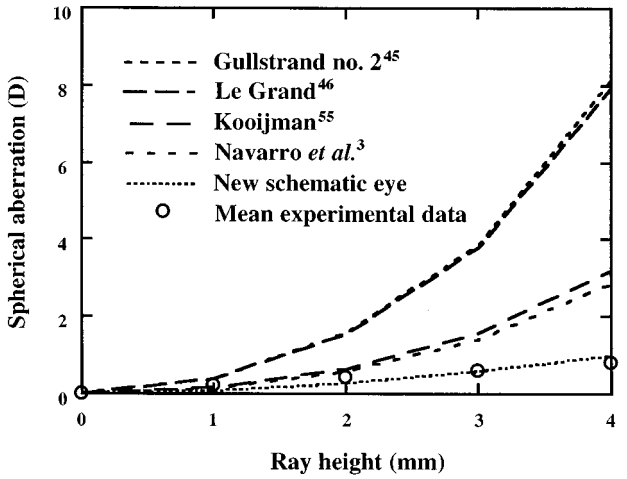

Fig. 5. Comparison of the spherical aberration predicted by the new schematic eye with spherical aberrations estimated by various paraxial and finite model eyes and the mean experimental results.

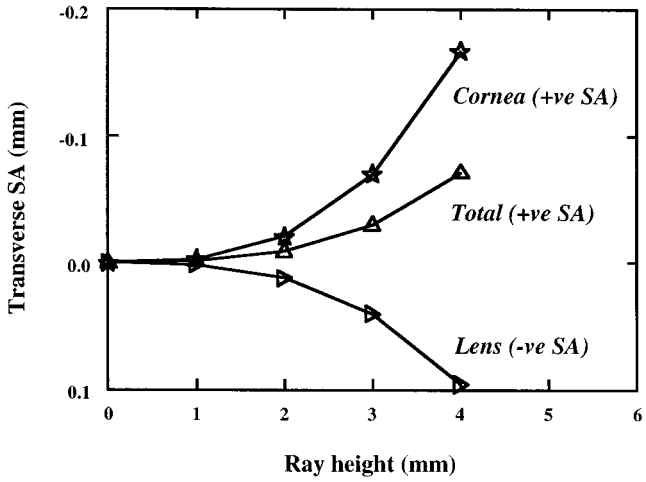

Fig. 6. Contribution of the gradient-index lens (GRIN) to the spherical aberration of the eye. Here $+ve\ SA$ and $-ve\ SA$ mean positive and negative spherical aberration, respectively.

(squared multiple correlation $R^2 = 0.98$). Data from Wald and Griffin,[57] Bedford and Wyszecki,[58] Howarth and Bradley,[59] and Cooper and Pease[60] are plotted in Fig. 7 for comparison with the longitudinal chromatic aberration predicted from the new model eye.

Sine-wave polychromatic modulation transfer functions of the new model eye were calculated for a 4-mm pupil and are shown in Fig. 8. The Stiles–Crawford effect is incorporated into the calculation by introducing a two-dimensional Gaussian apodization filter for the amplitude of the effect, as was done by van Meeteren.[1] This has the form $I = 10^{-(\alpha/2)w^2}$ where I is the intensity, $\alpha = 0.05$, and w is the radial distance from the pupil center in millimeters.[61] Polychromatic MTF's for an equienergy illuminant were calculated, taking into account the photopic spectral sensitivity function of retinal receptors (V_λ curve). The latter was simulated by using wavelengths of 510, 555, and 610 nm with weightings of 1, 2, and 1 respectively. Figure 8 compares the modulation transfer function calculated from the new model eye with the most recent experimental results of Artal *et al.*[62] and Navarro *et al.*[63]

6. DISCUSSION

Many finite schematic eyes proposed in the past were based on a previous paraxial schematic model and incorporated various refracting surfaces as required[3,54,55] or modified the lens into a gradient-index structure.[4,56] For these models, much of the original biometric data incorporated into the earlier paraxial model were retained. Given the vast amount of recently published biometric data, it is possible to develop a new model eye that incorporates data specifically collected with the most modern and accurate techniques. This means that errors due to limitations of the accuracy of outdated instruments are not propagated, and the new model accounts for changing trends in the population with respect to biometric data.

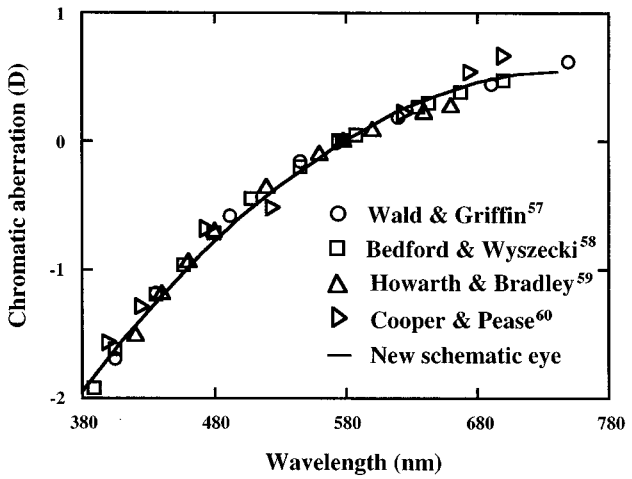

Fig. 7. Comparison of the chromatic aberration predicted by the new schematic eye with various experimental results.

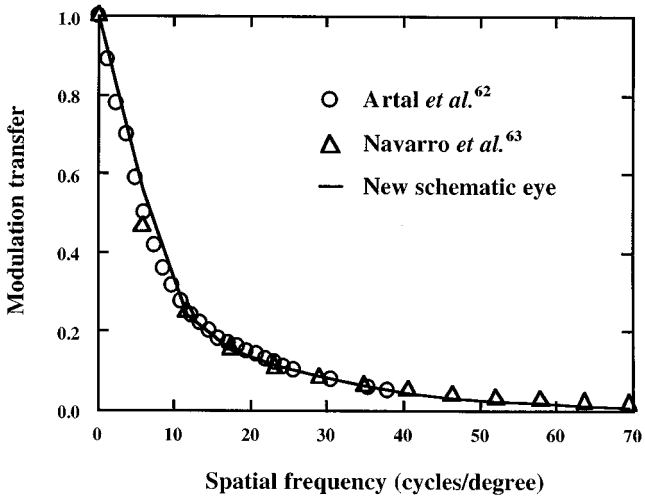

Fig. 8. Sine-wave polychromatic MTF for a 4-mm pupil calculated with horizontal gratings, compared with the most recent experimental data of Navarro *et al.*[63] and Artal *et al.*[62]

A. Anatomical Accuracy

The anatomical accuracy of a schematic eye is very important for the purpose of modeling vision in refractive procedures. We produced a model eye with all of the refracting surfaces represented, so that each individual parameter could be varied according to the refractive procedure applied (e.g., photorefractive keratectomy modifies the front surface of the cornea only, and an intraocular lens replaces the entire crystalline lens).

The equivalent power of the new model eye is 60.35 D. This is close to the currently accepted value of 60 D for the eye and is similar to those of other model eyes.[3–5,45,46,54–56] The axial length of the new model eye is 23.95 mm, which compares favorably with the average value of 24 mm for males and slightly less than 24 mm for females. Finite eyes such as those proposed by Lotmar,[54] Kooijman,[55] and Navarro *et al.*[3] were based on Le Grand's[46] paraxial model eye and had axial lengths of approximately 24.2 mm, slightly longer than values determined experimentally.

In comparison with other finite eyes, our new model eye attempts to be anatomically accurate while providing optical information about the human eye that is as close as possible to experimental results. Lotmar,[54] Kooijman,[55] and Navarro *et al.*[3] used aspheric refracting surfaces but did not incorporate a gradient-index lens. Blaker[56] adopted a gradient-index structure for the lens to describe accommodative changes but did not introduce asphericity in any refracting surfaces. Smith *et al.*[4] included both aspheric surfaces and a gradient-index lens. However, they based their model on the Gullstrand no. 1 eye. The equivalent power of their eye is therefore 58.64 D, less than the accepted 60 D; and the axial length for the eye is 24.35 mm, slightly longer than the average experimental value. Furthermore, they adopted positive asphericity values for the lens (7.9 and 2.6 for the anterior and posterior surfaces, respectively), which led to estimates of the spherical aberration of the eye that were higher than empirical values.

The aspheric shape of the posterior corneal surface in combination with the aspheric front surface provides a thickness of 0.50 mm to the central cornea and 0.91 mm at a peripheral point 6 mm from the center, the thickness gradually increasing from the center to the periphery. At 3 mm from the center, the thickness value is 0.62 mm, which compares favorably with measurements of peripheral corneal thickness by Hirji and Larke,[24] who found a thickness of 0.60 ± 0.05 mm and 0.57 ± 0.03 mm at 15° (approximately 3 mm) nasal and temporal to the center, respectively. This feature of the new model eye is more realistic than thickness values in previous finite schematic models,[3,4,54–56] as the peripheral cornea in these models are much thicker than that in empirical data owing to the spherical back surface adopted for the cornea.

As far as we know, the new proposed model eye is the first to incorporate both angle alpha and decentration of the pupil, thus distinguishing it from all previously published schematic eyes. Failure to incorporate angle alpha assumes coincidence of the visual and optical axes, which is anatomically inaccurate and may lead to optical inaccuracy.

Pupil decentration was included for anatomical accuracy of the representation of the eye. The decentration of the human pupil is taken to be 0.5 mm on average and therefore leads to slight transverse chromatic aberration (TCA). According to Thibos *et al.*[64] the magnitude of TCA present at the fovea can be approximated by the equation

$$\phi = h\Delta Rx, \tag{10}$$

where h is the pupil decentration in meters, ΔRx is the LCA in diopters, and ϕ is TCA in radians.

For the present model, this translates to a foveal TCA of approximately 1.2 arcmin for red and blue lights of wavelengths 605 and 497 nm, respectively. This compares favorably with results of Rynders *et al.*,[65] who found that the absolute magnitude of foveal TCA for any given individual was from 0.05 to 2.67 arcmin for red and blue lights of 605 and 497 nm, respectively. The mean foveal TCA of 85 young adults from their study was 0.8 arcmin.

B. Importance of the Gradient-Index Lens

A lens with a gradient-index (GRIN) structure was introduced in this new model to represent the anatomical structure of the human crystalline lens. Most previous finite schematic eyes either had aspheric refracting surfaces and a homogeneous lens[3,54,55] or a GRIN lens structure with spherical surfaces,[56] but not both.

The added complexity of GRIN is required in order to provide the functional power of the lens while keeping the realistic values of the refractive index of the lens. Previous schematic models with a homogeneous lens had to adopt a refractive as high as 1.42 for the lens in order to produce the functional power of the lens (approximately 20 D). However, the refractive index of the lens has been measured to vary from 1.386 in the cortex to 1.404 in the nucleus,[44] and these values can produce the power of the lens only if they are in the form of GRIN. This constitutes a major difference from previous schematic eye models (Smith *et al.*[4] used GRIN, but it does not compare favorably in modeling vision). It is also because of the GRIN lens that we were able to obtain a more empirically accurate value of the axial length for the new model eye without increasing the equivalent power.

C. Optical Performance

Spherical aberration predicted by the new model eye compares well with experimental results (see Fig. 5). This similarity is achieved by incorporating into the model eye a combination of aspheric surfaces for the posterior cornea and both the anterior and the posterior surfaces of the lens. Also, the gradient distribution of the lens index provides some negative spherical aberration to offset the positive spherical aberration that is due to the cornea (see Fig. 6). This matches the general view that the lens plays an important role in reducing the aberrations of the eye. El Hage and Berny[66] measured the aberration of one whole eye and the shape of its cornea and deduced that the lens must play a large compensatory role resulting in diminishing corneal aberration. This opinion was shared by Hartridge.[67] Jenkins[68] found that the cornea had about the same amount of aberration as the entire eye, thus implying that the lens is almost free of aberration. Results by Millodot and Sivak[69] showed that the aberration of the lens does not systematically neutralize that of the cornea. Of the 17 subjects for whom they measured lenticular spherical aberration, two had slight negative values, four showed no measurable amount, and the rest had positive values.

Most previous finite models[3,4,54–56] assumed the posterior cornea to be spherical. Although the posterior corneal surface does not play an important role in refracting rays, an aspheric surface has the effect of fine-tuning the spherical aberration of the eye at large ray heights from the optical axis in our model. Modifications of the parameters of the GRIN lens would also be very effective in altering the estimates of spherical aberration. However, we did not consider manipulating the parameters of the GRIN lens to match the spherical-aberration data from the literature, as this would defeat the goal of anatomical accuracy. The asphericity of the back surface of the cornea was chosen as the mechanism for fine-tuning the average spherical aberration of the eye instead, because we believe that it is the least well defined parameter of the eye. Individual changes in the parameters of the GRIN lens would most likely account for the large intersubject variability encountered in spherical-aberration measurements, as described above.

To account for the chromatic aberration of the eye, values for the dispersion of the ocular media were incorporated into the new model. The dispersion of the ocular media can be approximated by that of water, since results of chromatic aberration for wavelengths from 380 to 780 nm for the new model eye predict experimental measurements accurately, as seen from Fig. 4 ($R^2 = 0.98$). We did not choose to adopt dispersion measurements of the human ocular media,[47,48] because of the large errors involved in the measurements. In comparison, water was much better defined.

The sine-wave MTF calculated from our model eye compares favorably with the most recent experimental results[62,63] (see Fig. 8). The remarkably close agreement between our computed polychromatic MTF and the monochromatic MTF's measured by Artal *et al.*[62] and Navarro *et al.*[63] is surprising. One would expect the polychromatic MTF to be worse than the monochromatic one because of the effect of chromatic aberration on image quality. In this case, it is probable that the computed MTF results are better than expected because irregular aberrations of the eye have not been included in the model.

The incorporation of angle alpha and pupil decentration affects calculations of image quality. Angle alpha decreases the modulation sensitivity of a centered system, but the decentration of the pupil in the same direction offsets some of this effect, especially at low spatial frequencies. Modulation transfer functions estimated from other schematic eyes were not significantly higher than empirical results, even though they did not include angle alpha. This is probably because the spherical aberration in these model eyes was higher than in experimental results and therefore contributed to lower modulation sensitivities.

D. Future Research

While our new model eye predicts spherical and chromatic aberration of the eye, it is limited in its optical structures to those refracting surfaces that can be described mathematically. Further improvements of the model would include incorporation of irregular or nonrotationally symmetric surfaces. Such surfaces may not be representative of the general population but might be more useful for the purpose of assessing image-quality functions in individual eyes. This would be necessary to achieve the best result in modeling vision in individual eyes for purposes such as refractive surgery, where the characteristics of each person are unique. Additional biometric knowledge such as the curvature of the retina is also required for analysis of off-axis aberrations.

The present model does not yet account for changes with age, accommodation, or individual variability. Further research on the changes of ocular biometry with age is required for incorporation of this factor into the eye model. To extend the model further, we need to acquire more knowledge about the surface structure and distribution of the refractive index of the lens as well as how these change during accommodation. Although a schematic

eye represents an average model, it is possible to incorporate individual characteristics for the exact prediction of the visual performance of a given subject. Further research is necessary to improve and expand this model eye.

The spherical-aberration curve predicted by the new model eye has a somewhat parabolic shape, as expected from aberration theory, rather than the linear relationship indicated by empirical data. More detailed biometric data and empirical results for spherical aberration are necessary to investigate the deviations between experimental and calculated curves.

The new model eye presented here is based on experimental biometric data except for the posterior corneal asphericity and dispersion values due to lack of data. Careful compilation of experimental measurements produced quite successfully a finite schematic eye model. This shows that the various biometric measurements available are fairly accurate when carefully screened for the desired purpose. The posterior corneal asphericity and the gradient-index distribution of the lens were modeled for the new model eye to have an equivalent power of 60 D and an axial length of 24 mm and to predict spherical aberration. Future investigation into the empirical values of the above two parameters need to be performed in order to confirm the values obtained from the present modeling.

7. CONCLUSION

To the best of our knowledge, the new finite model eye presented in this paper is the first schematic eye model that predicts both chromatic and spherical aberrations of the eye within the tolerances of empirical results. Apart from providing optical parameters and serving as a vehicle for image-quality calculations, the new model can be considered to be a quasi-true anatomical representation of an average emmetropic human eye. Its close anatomical representation to the human eye makes it suitable for studies investigating visual performance under normal or altered conditions, such as reshaping of the cornea in refractive surgery, estimating vision where the cornea is distorted, changing the ocular refraction by application of contact lenses or spectacle lenses, and even implantation of intraocular lenses.

ACKNOWLEDGMENT

We thank M. C. Rynders and J. J. Vos for helpful comments on the manuscript.

REFERENCES AND NOTES

1. A. van Meeteren, "Calculations on the optical modulation transfer function of the human eye for white light," Opt. Acta **21**, 395–412 (1974).
2. H. L. Liou and N. A. Brennan, "The prediction of spherical aberration with schematic eyes," Ophthalmic. Physiol. Opt. **16**, 348–354 (1996).
3. R. Navarro, J. Santamaría, and J. Bescós, "Accommodation-dependent model of the human eye with aspherics," J. Opt. Soc. Am. A **2**, 1273–1281 (1985).
4. G. Smith, B. K. Pierscionek, and D. A. Atchison, "The optical modelling of the human lens," Ophthalmic. Physiol. Opt. **11**, 359–369 (1991).
5. M. Ye, X. X. Zhang, L. N. Thibos, and A. Bradley, "A new single-surface model eye that accurately predicts chromatic and spherical aberrations of the human eye," Invest. Ophthalmol. Visual Sci. (Suppl.) **34**, 777 (1993).
6. L. N. Thibos, M. Ye, X. X. Zhang, and A. Bradley, "The chromatic eye: a new reduced-eye model of ocular chromatic aberration in humans," Appl. Opt. **31**, 3594–3600 (1992).
7. L. N. Thibos, M. Ye, X. X. Zhang, and A. Bradley, "A new optical model of the human eye," Opt. Photon. News **4**, 12 (1993).
8. A. Bradley, School of Optometry, Indiana University, Bloomington, Ind. 47405-3201 (personal communication, 1995): corrections to the Ye *et al.* abstract (Ref. 5): The refracting surface defined as $Y = 0.0899X^2 + 0.0006X^4$ should be $Y = 0.0899X^2 + 0.0005X^4$ instead.
9. S. Stenström, "Investigation of the variation and the correlation of the optical elements of human eyes," Am. J. Optom. **25**, 340–350 (1948).
10. F. Jansson, "Measurements of intraocular distances by ultrasound," Acta Ophthalmol. Suppl. **74**, 1–49 (1963).
11. C. S. Yu, D. Kao, and C. T. Chang, "Measurement of the length of the visual axis by ultrasonography in 1789 eyes," Chin. J. Ophthalmol. **15**, 45–47 (1979).
12. J. F. Koretz, P. L. Kaufman, M. W. Neider, and P. A. Goeckner, "Accommodation and presbyopia in the human eye—aging of the anterior segment," Vision Res. **29**, 1685–1692 (1989).
13. D. A. Leighton and A. Tomlinson, "Changes in axial length and other dimensions of the eyeball with increasing age," Acta Ophthalmol. **50**, 815–826 (1972).
14. S. T. Fontana and R. F. Brubaker, "Volume and depth of the anterior chamber in the normal aging human eye," Arch. Ophthalmol. **98**, 1803–1808 (1980).
15. J. Larsen, "The sagittal growth of the eye," Acta Ophthalmol. **49**, 239–262 (1971).
16. R. Weekers and J. Grieten, "Mesure de la profondeur de la chambre antérieure en clinique," Soc. Belg. Ophthalmol. **129**, 361–381 (1961).
17. V. Clemmensen and M. H. Luntz, "Lens thickness and angle-closure glaucoma," Acta Ophthalmol. **54**, 193–197 (1976).
18. R. F. Lowe, "Central corneal thickness," Br. J. Ophthalmol. **53**, 824–826 (1969).
19. F. K. Hansen, "A clinical study of the normal human central corneal thickness," Acta Ophthalmol. **49**, 82–89 (1971).
20. E. L. Martola and J. L. Baum, "Central and peripheral corneal thickness," Arch. Opththalmol. **79**, 28–30 (1968).
21. P. S. Soni and I. M. Borish, "A report on central and peripheral corneal thickness," Int. Contact Lens Clin. **6**, 66–70 (1979).
22. D. M. Maurice and A. A. Giardini, "A simple optical apparatus for measuring the corneal thickness and the average thickness of the human cornea," Br. J. Ophthalmol. **35**, 169–177 (1951).
23. A. Tomlinson, "A clinical study of the central and peripheral thickness and curvature of the human cornea," Acta Ophthalmol. **50**, 73–82 (1972).
24. N. K. Hirji and J. R. Larke, "Thickness of human cornea measured by topographic tachometry," Am. J. Optom. Arch. Am. Acad. Optom. **55**, 97–100 (1978).
25. A. Sorsby, M. Sheridan, A. G. Leary, and B. Benjamin, "Vision, visual acuity and ocular refraction in young men," Brit. Med. J. **1**, 1394–1398 (1960).
26. A. Sorsby, B. Benjamin, J. B. Davey, M. Sheridan, and J. M. Tanner, *Emmetropia and Its Aberrations. A Study in the Correlation of the Optical Components of the Eye*. Medical Research Council Special Report Series No. 293 (Her Majesty's Stationary Office, London, 1957).
27. M. Townsley, "New knowledge of the corneal contour," Contacto **14**, 38–43 (1970).
28. R. B. Mandell and R. St. Helen, "Mathematical model for the corneal contour," Br. J. Physiol. Opt. **26**, 183–197 (1971).
29. P. H. Kiely, G. Smith, and G. Carney, "The mean shape of the human cornea," Opt. Acta **29**, 1027–1040 (1982).

30. B. A. J. Clark, "Variations in corneal topography," Aust. J. Optom. **56**, 399–413 (1973).
31. M. Guillon, P. M. Lydon, and C. Wilson, "Corneal topography: a clinical model," Ophthalmic. Physiol. Opt. **6**, 47–56 (1986).
32. R. F. Lowe and B. A. Clark, "Posterior corneal curvature," Br. J. Ophthalmol. **57**, 464–470 (1973).
33. J. M. Royston, M. C. M. Dunne, and D. A. Barnes, "Measurement of the posterior corneal radius using slit lamp and Purkinje image techniques," Ophthalmic. Physiol. Opt. **10**, 385–388 (1990).
34. M. C. M. Dunne, J. M. Royston, and D. A. Barnes, "Normal variations of the posterior corneal surface," Acta Ophthalmol. **70**, 255–261 (1992).
35. A. G. Rivett and A. Ho, "The posterior corneal topography," Invest. Ophthalmol. Visual Sci. (Suppl.) **32**, 1001–1001 (1991).
36. S. Patel, J. Marshall, and F. W. Fitzke, "Shape and radius of posterior corneal surface," Refract. Corneal Surg. **9**, 173–181 (1993).
37. R. F. Lowe, "Anterior lens curvature," Br. J. Ophthalmol. **56**, 409–413 (1972).
38. R. F. Lowe and B. A. J. Clark, "Radius of curvature of the anterior lens surface," Br. J. Ophthalmol. **57**, 471–474 (1973).
39. N. Brown, "The change in lens curvature with age," Exp. Eye Res. **19**, 175–183 (1974).
40. M. J. Howcroft and J. A. Parker, "Aspheric curvatures for the human lens," Vision Res. **17**, 1217–1223 (1977).
41. C. Roberts, "The accuracy of 'power' maps to display curvature data in corneal topography systems," Invest. Ophthalmol. Visual Sci. **35**, 3525–3532 (1994).
42. S. Nakao, T. Ono, R. Nagata, and K. Iwata, "The distribution of refractive index in the human crystalline lens," Jpn. J. Clin. Ophthalmol. **23**, 903–906 (1969).
43. M. C. W. Campbell, "Measurement of refractive index in an intact crystalline lens," Vision Res. **24**, 409–415 (1984).
44. B. K. Pierscionek and D. Y. C. Chan, "Refractive index gradient of human lenses," Optom. Vis. Sci. **66**, 822–829 (1989).
45. A. Gullstrand, *Helmholtz's Physiological Optics* (Optical Society of America, New York, 1924), Appendix, pp. 350–358.
46. Y. Le Grand, *Physiological Optics* (Springer-Verlag, New York, 1980), pp. 54–55.
47. D. A. Palmer and J. Sivak, "Crystalline lens dispersion," J. Opt. Soc. Am. **71**, 780–782 (1981).
48. J. G. Sivak and T. Mandelman, "Chromatic dispersion of the ocular media," Vision Res. **22**, 997–1003 (1982).
49. G. Westheimer, "Image quality in the human eye," Opt. Acta **17**, 641–658 (1970).
50. M. A. Wilson, M. C. W. Campbell, and P. Simonet, "Change of pupil centration with change of illumination and pupil size," Optom. Vis. Sci. **69**, 129–136 (1992).
51. G. Walsh, "The effect of mydriasis on the pupillary centration of the human eye," Ophthalmic. Physiol. Opt. **8**, 178–182 (1988).
52. G. Walsh and W. N. Charman, "The effect of pupil centration and diameter on ocular performance," Vision Res. **28**, 659–665 (1988).
53. A. G. Bennett and R. B. Rabbetts, *Clinical Visual Optics*, 2nd ed. (Butterworth-Heinemann, Oxford, 1989), pp. 17–18.
54. W. Lotmar, "Theoretical eye model with aspherics," J. Opt. Soc. Am. **61**, 1522–1529 (1971).
55. A. C. Kooijman, "Light distribution on the retina of a wide-angle theoretical eye," J. Opt. Soc. Am. **73**, 1544–1550 (1983).
56. J. W. Blaker, "Toward an adaptive model of the human eye," J. Opt. Soc. Am. **70**, 220–223 (1980).
57. G. Wald and D. R. Griffin, "The change in refractive power of the human eye in dim and bright light," J. Opt. Soc. Am. **37**, 321–336 (1947).
58. R. E. Bedford and G. Wyszecki, "Axial chromatic aberration of the human eye," J. Opt. Soc. Am. **47**, 564–565 (1957).
59. P. A. Howarth and A. Bradley, "The longitudinal chromatic aberration of the human eye, and its correction," Vision Res. **26**, 361–366 (1986).
60. D. P. Cooper and P. L. Pease, "Longitudinal chromatic aberration of the human eye and wavelength in focus," Am. J. Optom. Physiol. Opt. **65**, 99–107 (1988).
61. R. A. Applegate and V. Lakshminarayanan, "Parametric representation of Stiles–Crawford functions: normal variation of peak location and directionality," J. Opt. Soc. Am. A **10**, 1611–1623 (1993).
62. P. Artal, M. Ferro, I. Miranda, and R. Navarro, "Effects of aging in retinal image quality," J. Opt. Soc. Am. A **10**, 1656–1662 (1993).
63. R. Navarro, P. Artal, and D. R. Williams, "Modulation transfer of the human eye as a function of retinal eccentricity," J. Opt. Soc. Am. A **10**, 201–212 (1993).
64. L. N. Thibos, A. Bradley, and X. X. Zhang, "Effect of ocular chromatic aberration on monocular visual performance," Optom. Visual Sci. **68**, 599–607 (1991).
65. M. Rynders, B. Lidkea, W. Chisholm, and L. N. Thibos, "Statistical distribution of foveal transverse chromatic aberration, pupil centration, and angle ψ in a population of young adult eyes," J. Opt. Soc. Am. A **12**, 2348–2357 (1995).
66. S. G. El Hage and F. Berny, "Contribution of the crystalline lens to the spherical aberration of the eye," J. Opt. Soc. Am. **63**, 205–211 (1973).
67. H. Hartridge, *Recent Advances in the Physiology of Vision* (Churchill, London, 1950), pp. 78–84.
68. T. C. A. Jenkins, "Aberrations of the eye and their effects on vision: part 1," Br. J. Physiol. Opt. **20**, 59–91 (1963).
69. M. Millodot and J. Sivak, "Contribution of the cornea and lens to the spherical aberration of the eye," Vision Res. **19**, 685–687 (1979).
70. J. A. Parker, "Aspheric optics of the human lens," Can. J. Ophthalmol. **7**, 168–175 (1972).